

Contents lists available at ScienceDirect

Cleaner Materials

journal homepage: www.journals.elsevier.com/cleaner-materials





Evaluation of strength, durability, and microstructure characteristics of slag-sand-induced concrete

Reshma T.V.^{a,b,*}, Chandan Kumar Patnaikuni^c, Tanu H.M.^d, Bharath A.^a

- ^a Assistant Professor, Department of Civil Engineering, GITAM School of Technology, GITAM University, Bengaluru, Karnataka, India
- ^b Research Scholar, Department of Civil Engineering, GITAM School of Technology, GITAM University, Visakhapatnam, Andhra Pradesh, India
- ^c Professor, Department of Civil Engineering, GITAM School of Technology, GITAM University, Visakhapatnam, Andhra Pradesh, India
- ^d Assistant Professor, Department of Civil Engineering, Ballari Institute of Technology and Management, Ballari, Karnataka, India

ARTICLE INFO

Keywords: Durability Mechanical properties Microstructure Slag sand concrete Regression analysis Cost analysis

ABSTRACT

This paper focused on the usage and behavior of slag sand by investigating the fresh, mechanical, durability, and microstructural properties of M40 grade concrete. However, in India, more research on the effect of slag on mechanical strength is needed with in-depth microstructure & durability investigation. To fill this research gap and promote slag sand usage, a systematic and scientific investigation was conducted in which 9 concrete mixes with partial and total replacement of fine aggregate with slag sand were prepared. Compressive, split tensile strength & UPV tests are performed at 3, 7, 28, and 90 days of curing to know the mechanical properties. Linear regression analysis is done to correlate and predict the strength of concrete using different mechanical properties. According to test results, workability and mechanical properties improve with the increase in the replacement of slag sand. Slag sand concrete forms a dense network at an optimum replacement achieving Maximum rise in strength of about 17 to 33 %, referring to the control mix resulting in an environmentally friendly material. Thereby reducing the disposal of industrial effluent. Conversely, increased replacement beyond 40 % of slag sand in concrete caused a reduction in the slump and mechanical properties with increased curing age. Microstructure results revealed the formation of CSH, CASH, ettringite, calcite, and good bonding with an aggregate. Slag sand tends to absorb more water with its increased percentage due to its shape, texture, and surface area, as evidenced in its SEM images & workability. The durability of slag sand concrete has performed better and is economically feasible than M-sand mixed concrete. Hence, recycling slag sand in concrete yields an economical, eco-friendly material and proves to be a robust substrate for various construction activities in sustainable waste management.

Introduction

Concrete is one of the most commonly used construction material and its manufacture leads to the economic growth of any country (H.M. and Unnikrishnan, 2022; Li et al., 2023) Aggregates are the inert materials rich in silica, calcium, magnesium, and other minerals that act as filler material and yield good bonding between cement and aggregates. Sustainability must be introduced in the industrial and construction sectors when using new raw materials and during production (Gencel et al., 2021). One of the most significant industries in the world is the

production and manufacture of steel materials. Different industrial processes that involve other raw materials produce additional waste (Jiang et al., 2022; Lu et al., 2023c). Steel slag is the primary waste material produced in these materials' manufacturing processes in terms of volume (Jiang et al., 2018; Nalon et al., 2022; Santhosh et al., 2021; Zhang et al., 2021). India is now the world's second-largest steel producer, behind China, with a historic high annual production of 120 million tonnes. The top ten countries by percentage of steel production in 2022 are shown in Fig. 1. Studies show that less than 30 % of steel slag is used in China, which creates more opportunities for waste recycling

Abbreviations: ANOVA, Analysis of variance; CASH, Calcium aluminate silicate hydrate; CH, Calcium hydroxide; CS, Compressive strength; CSH, Calcium silicate hydrate; C₂S, Dicalcium silicate; DOF, Degree of freedom; EDS, Energy dispersive X-ray spectroscopy; ITZ, Inter-facial transition zone; Rs, Rupees; SEM, Scanning electron microscopy; SS, Slag Sand; SNF, Sulphonated Naphthalene Formaldehyde; TS, Tensile strength; UHPC, Ultra high-performance concrete; UPV, Ultrasonic pulse velocity; XRD, X-Ray Diffraction.

E-mail addresses: rvishwes@gitam.edu (T.V. Reshma), ppatnaik@gitam.edu (C. Kumar Patnaikuni), tanoohm@gmail.com (H.M. Tanu), bashu@gitam.edu (A. Bharath).

https://doi.org/10.1016/j.clema.2023.100212

Received 17 August 2023; Received in revised form 16 November 2023; Accepted 27 November 2023 Available online 1 December 2023

2772-3976/© 2023 The Author(s). Published by Elsevier Ltd. This is an open access article under the CC BY-NC-ND license (http://creativecommons.org/licenses/by-nc-nd/4.0/).

Corresponding author.

and research to prevent waste dumping and environmental pollution (X. Wang et al., 2022). Recycling steel industry waste must be prioritized to encourage sustainable construction practices in India (Lu et al., 2023a, 2023d).

Slags have a lot of potential for use in the construction, cement manufacturing, wastewater, and water treatment industries, among other fields, including transportation. The various uses for steel slag show that it can be used well rather than being dumped in a landfill. Slags can be used in agriculture as fertilizers and soil acidity correctors. Due to the neutralizing effects of SiO₂, slags are composed of magnesium and calcium silicates. In addition, steel slags have been employed as a cheap source of Si to supply rice plants. Cold slag is used in steel plants for both internal consumption and external sale. After cooling, the slag is crushed and used as railway ballast and road metal (Jiang et al., 2023; Lu et al., 2023b; Teja et al., 2020). Due to the enormous demand in the concrete industry, using steel slag as supplementary cementitious materials, fine or coarse aggregates, or both is a viable option (L. Mo et al., 2020). Typically, aggregate makes up more than 60 % of the volume of concrete. Therefore, a promising method that could use steel slag on a large scale is to use it in concrete as a partial replacement for natural coarse or fine aggregates.

Steel slag powder's impact on the mechanical and durability qualities of cementitious materials was researched by Teng et al., 2013). The findings demonstrated that the steel slag significantly speeds up the hydration reaction of the composite, giving concrete its early and enhanced strength and durability properties. The impact of steel slag powder on the microstructure, mechanical, and volume properties of ultra-high-performance concrete (UHPC) was investigated by Zhang et al representing retarded early age hydration and reduced shrinkage over a period of time (Zhang et al., 2019). According to Kourounis et al., (Kourounis et al., 2007) steel slag's low calcium silicate content and C₂Srich morphology cause it to hydrate blended cement more slowly. Steel slag can also be used to create composites based on cement. Using a mercury porosimetry test, Lai et al. (Lai et al., 2021) examined the microstructure of concrete containing steel slag aggregate. According to the authors, steel slag increased concrete strength and decreased porosity. Concrete's wet packing density can be raised by adding steel slag powder. According to the findings, fine steel slag had less impact on the compressive strength, pore structure, and shrinkage characteristics of UHPC. Most of the cement particles in its inter-facial transition zone (ITZ) were loosely accumulated on the aggregate's generally flat surface. According to Arribas et al. (Arribas et al., 2015) the ITZ of steel slag concrete decreased by 50 %. Because steel slag aggregates absorb much

water, researchers frequently add water reducers to concrete to make it easier to work with (Xue et al., 2022a). However, micro level investigation is required considering various percentage of replacement and its properties. In the present study, slag sand, a steel industry by-product produced by JSW steel plant Ballari, replaces fine aggregate with slag sand. Microstructure, fresh, mechanical and durability properties are investigated to determine their optimum replacement level to minimize the disposal challenge and pollution in an environment. The following section describes the novelty and research significance of the study.

Novelty and research significance

India recently, gaining its attention for promoting sustainable materials for the construction. Few studies were done on mechanical properties, but detailed investigations on material, microstructure, mechanical and durability properties are needed to catch up. Identifying this gap in the research, steel industry refined waste, named slag sand (SS), is experimented with, and investigated systematically by using it in concrete as a replacement for artificial sand. Microstructure tests have evaluated Slag sand's basic structure and elemental components with manufactured sand.

A detailed investigation of the microstructure, strength, durability properties of SS incorporated concrete was studied by varying its percentage ranging from 0 to 100 %. After analysing and interpreting results for 3, 7, 28, and 90 days of curing, an optimum replacement of SS in concrete is concluded for the practical usage of waste. And the correlation with the concrete's properties and strength prediction with accuracy is emphasized through the linear regression analysis method. This research addresses the significant economic concern by promoting the usage of slag sand in construction materials. Thus, it can lead to ecofriendly, sustainable cement concrete production for all construction activities. The following section describes the details of the ingredients used in the concrete mix and their physical, chemical, and microstructure test results.

Materials

In concrete, Portland pozzolana cement having grade 53 that complies with Indian Standard IS:12269–2019 is used as a binder. The cement's initial and final setting times are 45 min and 565 min, respectively, with a consistency of 33 %. Cement has a specific gravity of 3.09, is 8 % finer than water, and is 9 % sound. Fig. 3 represents the SEM image of cement used in the study. Sand that has been manufactured,

Country wise Steel production in 2022

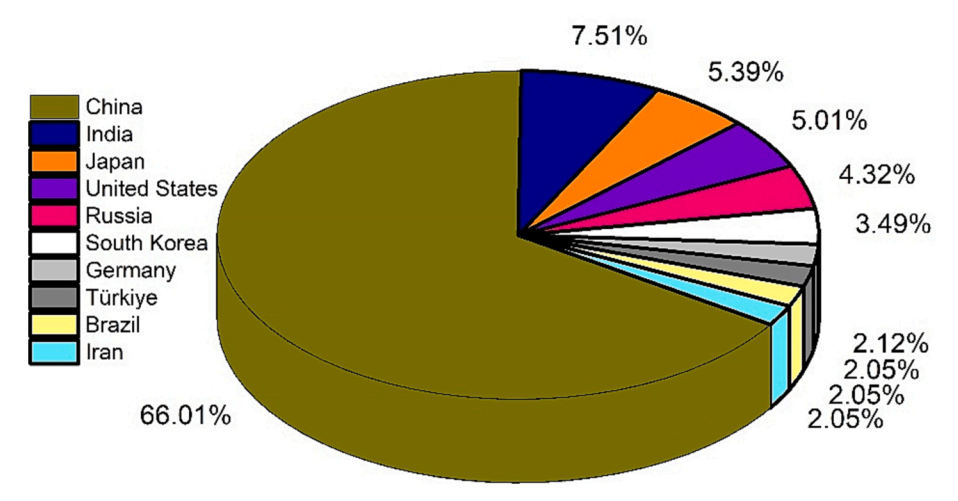


Fig. 1. Top 10 countries steel production during 2022.



Fig. 2. Concrete ingredients: a) Cement b) Slag sand c) Artificial sand d) Coarse aggregate.

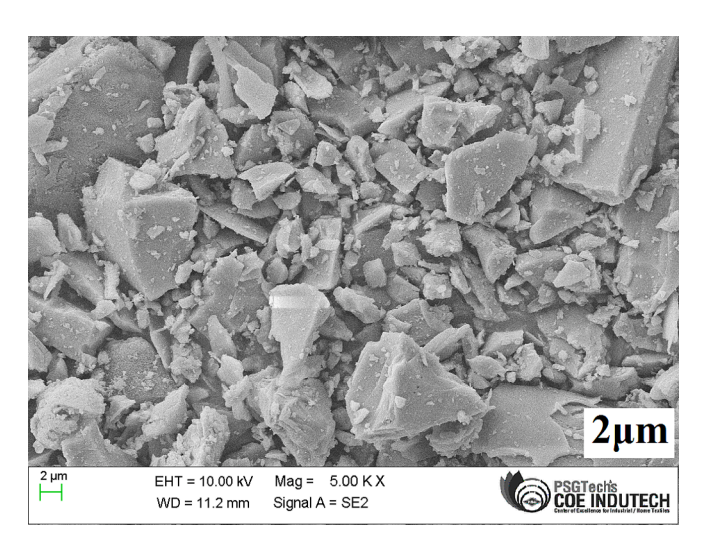


Fig. 3. SEM of Portland pozzolana cement.

also known as artificial sand, is made by crushing rock fragments into powder in a quarry. Slag sand, a steel by-product obtained from the JSW steel plant in Ballari, is combined with M-sand in varying amounts (T.V. and Chandan Kumar, 2023). The water absorption of artificial sand and slag sand are found to be 2.3 % and 4.06 % respectively which results in the increased water absorption of industrial by-product. XRD of slag sand and artificial sand depicts the presence of calcium magnesium divanadate, Zinc tetraphosphide, strontium bismuth oxide and quartz respectively at a 2-theta angle ranging from 20° to 40° as shown in Fig. 4. SEM images in Fig. 5 of slag sand and artificial sand reveals the similar angular, spherical, and flaky shape with rough texture. The size of the fine aggregates corresponding to zone-II are chosen. Coarse aggregate with solid and dense structures free from 12 mm and 20 mm impurities are used to prepare M40 grade concrete. Coarse aggregate, Artificial sand, and Slag sand have respective relative densities of 2.67, 2.58 and 2.54 g/cm³. Chemical admixture of SNF superplasticizer is used in the concrete mix of about 0.6 % by the weight of cement. Fig. 2 presents the major ingredients of concrete used in the experiment. Section 4 describes the mix design and concrete preparation employed in the experimental study.

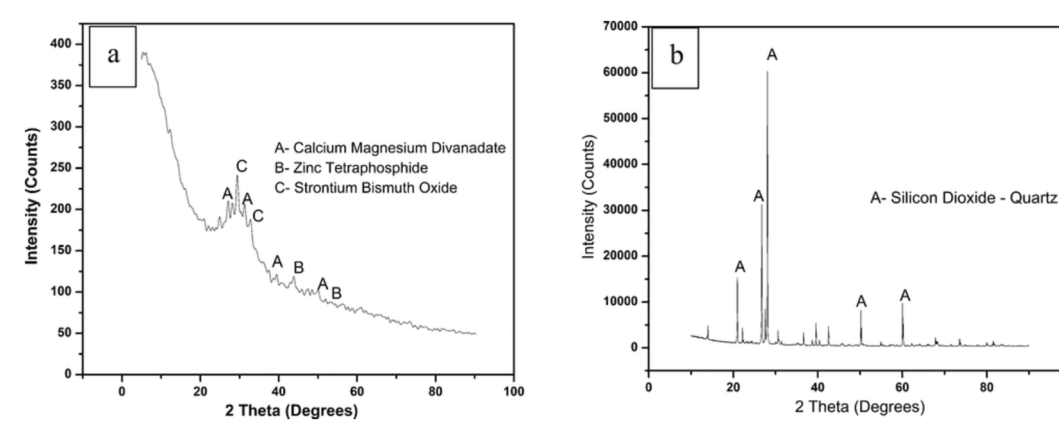


Fig. 4. XRD of a) slag sand and b) artificial sand.

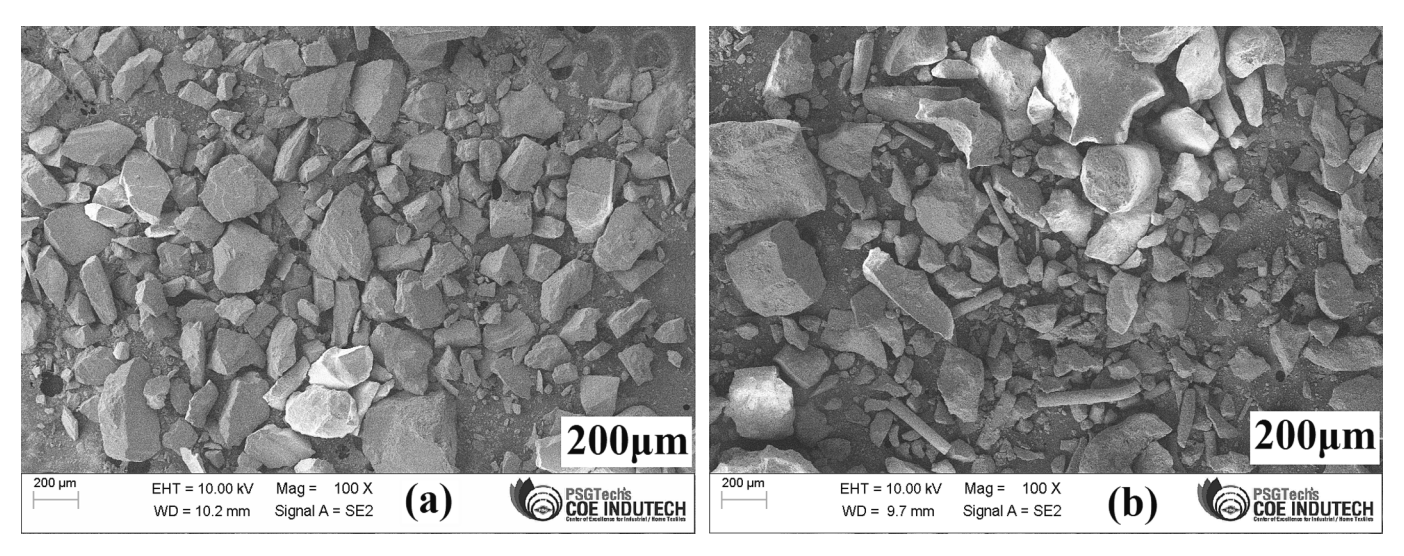


Fig. 5. SEM image of (a) slag sand and (b) artificial sand.

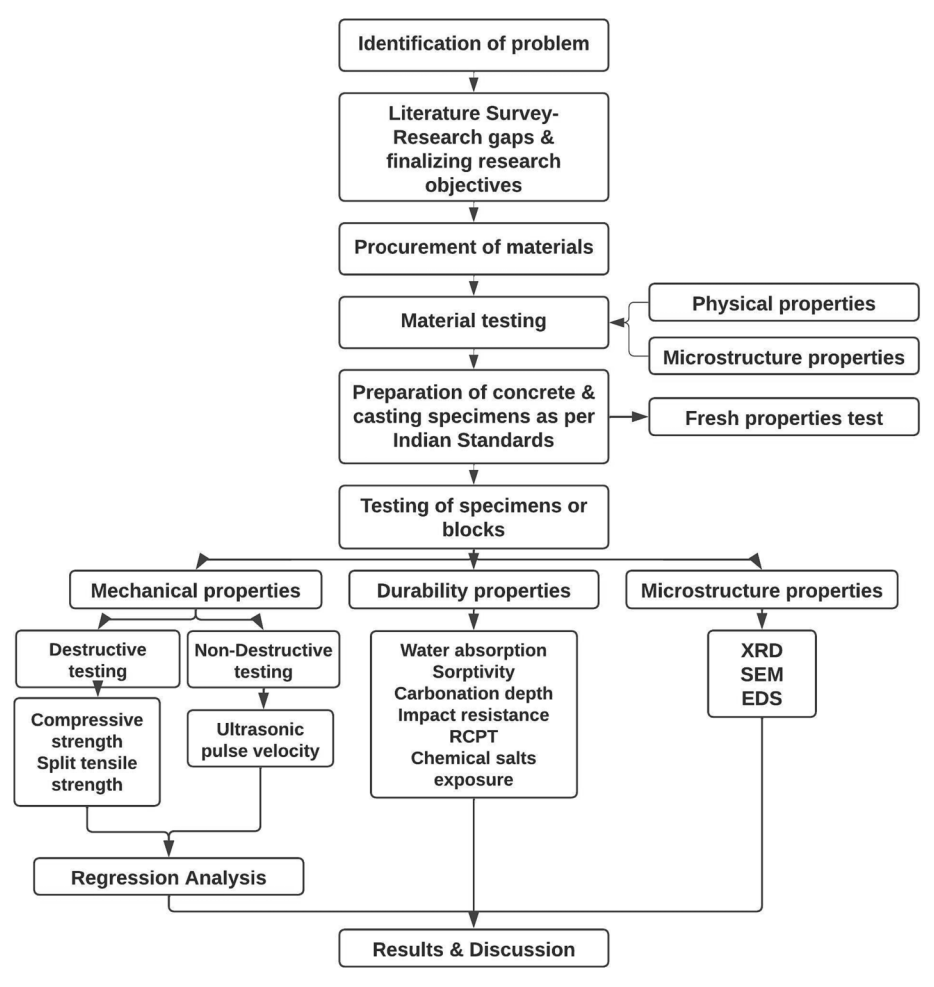


Fig. 6. Research methodology employed in the study.

Mix design and concrete preparation

Concrete mix design is prepared as per IS 10262–2019 for M40 grade of concrete. 0.38 is taken as water cement ratio as per the above mentioned IS code. Five different mixes were prepared with replacing m-sand with slag sand in M40 grade of concrete. The constant value of 388.18 kg/m 3 cement and superplasticizer content of 2.328 kg/m 3 is

used as an admixture to enhance the workability of concrete. Mixes are designed as MS-0, MS-25, MS-50, MS-75, and MS-100 in which M—sand is replaced with slag sand (0 %, 20 %, 25 %, 30 %, 40 %, 50 %, 60 %, 75 %, and 100 %). Maximum fine aggregate constant 489 kg/m³ and coarse aggregate constant 1173 kg/m³. These mixes were casted into specific dimensions for testing of compressive and split tensile strength. After obtaining Maximum failure load at 25 % replacement and marginal

decrement in 50 % replacement, additional four mixes were prepared to obtain the optimum mix of concrete. MS-20, MS-30, MS-40, MS-60 with slag sand 20 %, 30 %, 40 %, and 60 % were tried to determine the optimum percentage replacement of slag sand in the concrete mixes. These specimens are dried and tested after 3, 7, 28, and 90 days of water curing at room temperature $26+/-2^{\circ}$ C. Table 1 represents the mix design calculations of concrete. Fig. 7 represents the preparation, casting and testing of slag sand induced concrete specimens. The following section 5 describes the research methodology considered in the entire study. Also, its subsections narrate the detailed procedure of conducting fresh, mechanical, microstructure, and durability tests.

Experimental programme

Fresh properties

Slump cone test and compaction factor tests are performed to determine the workability of concrete as per the guidelines of Indian standard IS: 1199 (Part-VI)-2018(Reshma et al., 2021).

Mechanical properties

Cubes are cast to assess the compressive strength (CS) of concrete in accordance with IS: 516–1959. 150 mm \times 150 mm \times 150 mm cube is casted and tested for compressive load till failure as per the guidelines of IS: 516–1959 at 3, 7, 28 and 90 days of curing (IS 516, 1959). The testing is done using compression testing machine (CTM) having capacity of 2000 kN. Three cubes are checked after 3, 7, 28 and 90 days of water curing with each combination. Similarly, 150 mm diameter and 300 mm height cylindrical specimen is casted and tested on diametrical axis till failure as per the guidelines of IS: 516-1959 at 3, 7, 28 and 90 days of water curing. The testing is done using universal testing machine having capacity of 600 kN. Three cylinders were created for each combination and measured on different days to determine tensile strength (TS). Initially 0, 25, 50, 75, 100 % replaced specimens were investigated for strength. After noticing a Maximum strength at 25 %, we decided to investigate additional mixes with 20, 30, 40, 60 % replacement of slag sand to obtain an optimum mix proportion. A total of 216 specimens have been cast in this study. Among them, for the determination the compressive strength, and Ultrasonic pulse velocity (UPV), 108 cubes of 150 mm dimension are tested for travel time of electronic waves before application of compressive load on CTM. Similarly, for knowing the tensile strength of a concrete 108 specimens are tested. These experimental processes are done according to the Indian standards IS-13311–1992(part 1). The methodology of the research is as represented in Fig. 6.

Microstructure properties

Scanning electron microscopy (SEM) and Energy dispersive X-ray spectroscopy (EDS) is conducted using CARL ZEISS Sigma with Gemini Column having resolution of 1.5 nm and BRUKER Nano X-Flash Detector machine (Xue et al., 2022b). The concrete specimens cured for 28 days

are tested for strength and then the core sample size around 5 mm is chosen for SEM testing to rate the polymerization and structural elements in the matrix mix. The X-Ray diffraction (XRD), based on Bragg's law was conducted on various concrete mixes that are cured for 28 days. XRD analysis is performed for the powdered sample obtained after crushing the concrete specimen and sieved using 900 μm with Panalytical-Xpert³ diffractometer model. The range of 20 (theta) varied from 5° to 90° at a scanning rate of 4.02°/min with a 0.013° rate of increment.

Durability properties

Durability tests are performed on concrete to evaluate the permeability, resistance to environmental factors, carbonation, and tendency to crack. Rapid chloride ion penetration, carbonation depth, water absorption, sorptivity, impact resistance, and chemical salt exposure are performed to evaluate the quality and performance of concrete as per the Indian standards (K. H. Mo et al., 2020).

Section 6 and its subsections explain the results obtained from the testing, its detailed analytical discussion of the results, and its validation from the research articles. Section 7 describes the correlation of fresh and mechanical properties test results with the variation of SS and other influencing parameters.

Result and discussion

Workability

Medium & high workability with true and shear slump is noticed in slag sand incorporated concrete. Fig. 8 represents the test results variation of fresh properties of all nine mixes composed of slag sand from 0 to 100 %. From the test results, an improvement is observed in slump & compaction with increase in slag sand content. There is an increment in the fresh properties' performance up to 40 % replacement of slag sand from 90 to 112 mm. Workability of concrete increases with increase in slag sand due to many reasons. One of the main reasons is water binder ratio, type of precursors employed, filler materials and type of curing. Beyond 40 % of replacement, there is a marginal decrease in slump value from 112 to 91 mm indicating flash absorption of water from slag sand and weak porous structure and less dense concrete mix. SEM images reveals the presence of dense structure of Calcium silicate hydrate (CSH), Calcium aluminate silicate hydrate (CASH), Calcium hydroxide (CH) formation and increased slag results in porous structure. Similar observation is depicted by Sithole et al. (Sithole et al., 2022) on using slag as replacement material. But still all the mixes prepared using slag sand provides good workability for placing and shows better compaction.

Similar trend has been noticed from compaction factor test results as depicted in Fig. 8. Thus, we can conclude that slag sand performs better by providing workable concrete for its usage. Also, slag sand tends to absorb more water due to its size and surface texture compared to artificial sand. This can be evidenced from SEM image of slag sand and artificial sand as shown in Fig. 5, we can notice the size and shape of the

Table 1Mix design calculations per cubic meter of concrete (kg/m³).

Mix ID	Cement	M Sand	Slag Sand	Coarse Aggregate	Water	Admixture
MS-0	388.18	489	0	1173	47.51	2.328
MS-20		391.2	97.8			
MS-25		366.75	122.25			
MS-30		342.3	146.7			
MS-40		293.4	195.6			
MS-50		244.5	244.5			
MS-60		195.6	293.4			
MS-75		122.25	366.75			
MS-100		0	489			



Fig. 7. Preparation of concrete and specimens.

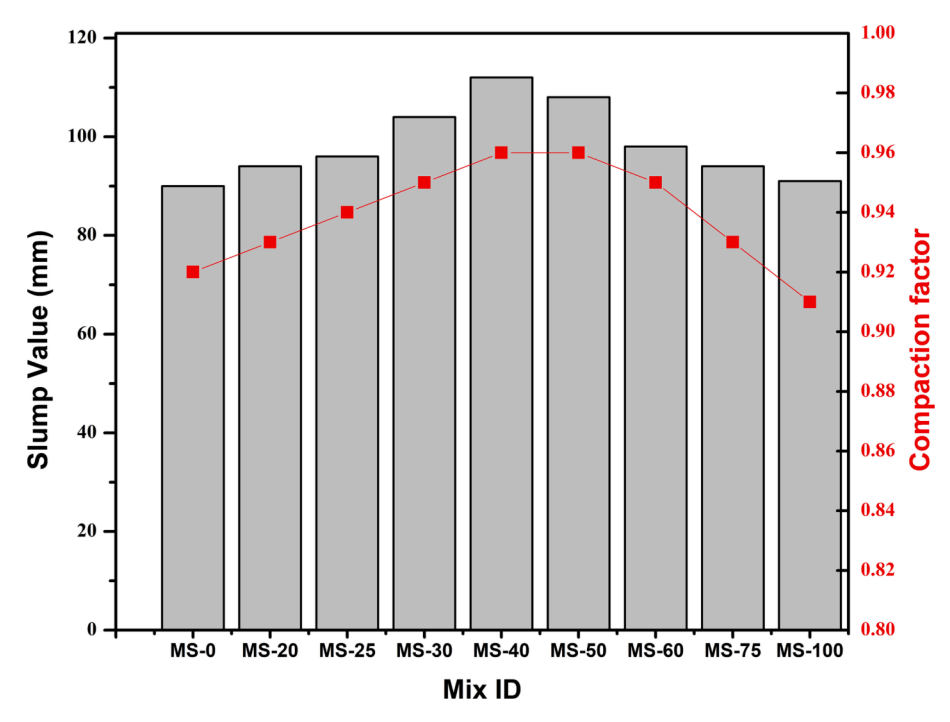


Fig. 8. Graphical representation of workability test results.

particles. Slag sand tends to possess finer particles with increased surface area. This results in the more absorption of water compared to artificial sand.

Compressive strength

From the test values, we calculated an average and standard deviation that is clearly represented in Fig. 9. We have noticed an error bar that indicated variation of compressive strength due to variation in water absorption and porous nature of SS. The consistency & stability of values is obtained with an increased age of curing. Maximum strength of 64 MPa & 67.56 MPa is achieved at a replacement of 40 % slag sand with an artificial sand in concrete mix at 28 and 90 days of curing. About

32.47 % and 27.3 % rise in CS is observed for MS-40 (40 % slag sand) in comparison to control mix (MS-0) after 28 and 90 days of curing. Highest strength is obtained due to the formation of dense structure with CSH, CASH and CH formation as revealed from the microstructural test results. With an increased slag sand, the strength starts declining due to porous structure and increased water absorption. Increased water absorption is noticed with increase slag sand content from the water absorption test. Similar trend of increased water absorption is noticed with slag as evidenced by Q. Yu et al. (Yu et al., 2023) and Lai et al. (Lai et al., 2022). But all the replaced concrete mixes have shown better results than the target strength required for the M40 grade mix concrete. The detailed investigation for obtaining the strength variation in slag sand concrete is interpretated using microstructural analysis.

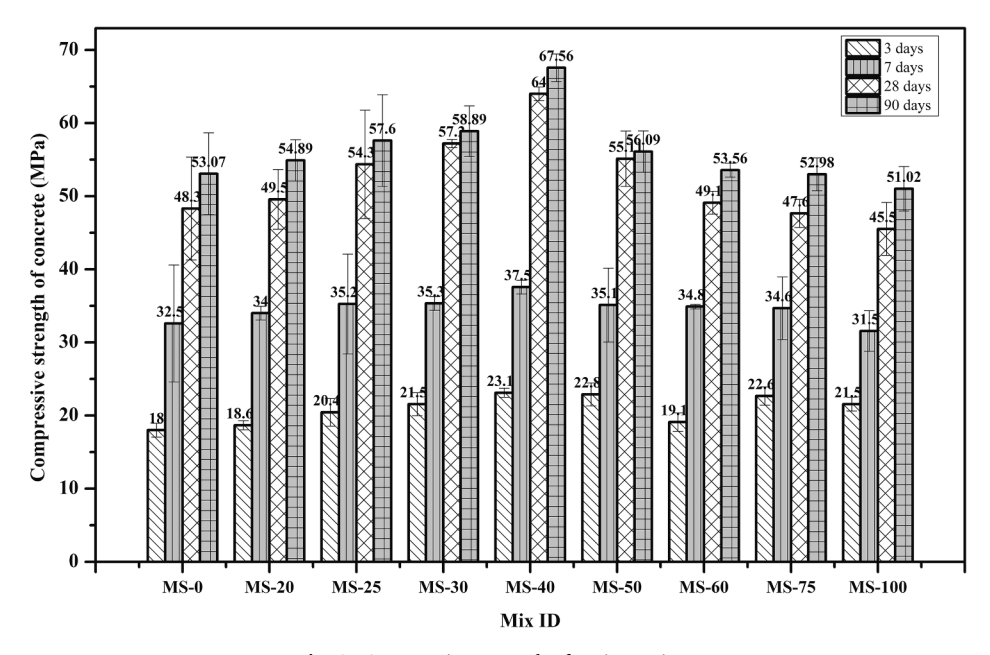


Fig. 9. Compressive strength of various mixes.

Split tensile strength

From the test values, we calculated an average and standard deviation that is clearly represented in Fig. 10. We have noticed an error bar that indicated variation of compressive strength due to variation in water absorption and compacted nature of slag sand. The consistency in values is obtained with an increased age of curing. Maximum strength of 4.38 MPa & 4.86 MPa is achieved at a replacement of 40 % slag sand with an artificial sand in concrete mix at 28 and 90 days of curing. About 16.22 % and 18 % rise in TS is observed for MS-40 (40 % slag sand) in comparison to control mix (MS-0) after 28 and 90 days of curing. Increased strength is the result of formation of dense structure and strong matrix between water binder content. Microstructure images

reveals the presence of quartz, CSH, ettringite, portlandite that resulted in an increased strength of slag induced concrete. With an increased slag sand, the strength starts declining due to porous structure and increased water absorption. Similar trend is observed by Q. Yu et al. (Yu et al., 2023) and Lai et al. (Lai et al., 2022) in their experimentation on slag replacement in the concrete mix. But all the replaced concrete mixes have shown better results than the target strength required for the M40 grade mix concrete (Mocharla et al., 2022). The detailed investigation for obtaining the strength variation in slag sand concrete is interpretated using microstructural analysis and linear regression analysis is performed to predict the equation and evaluate the accuracy of test results.

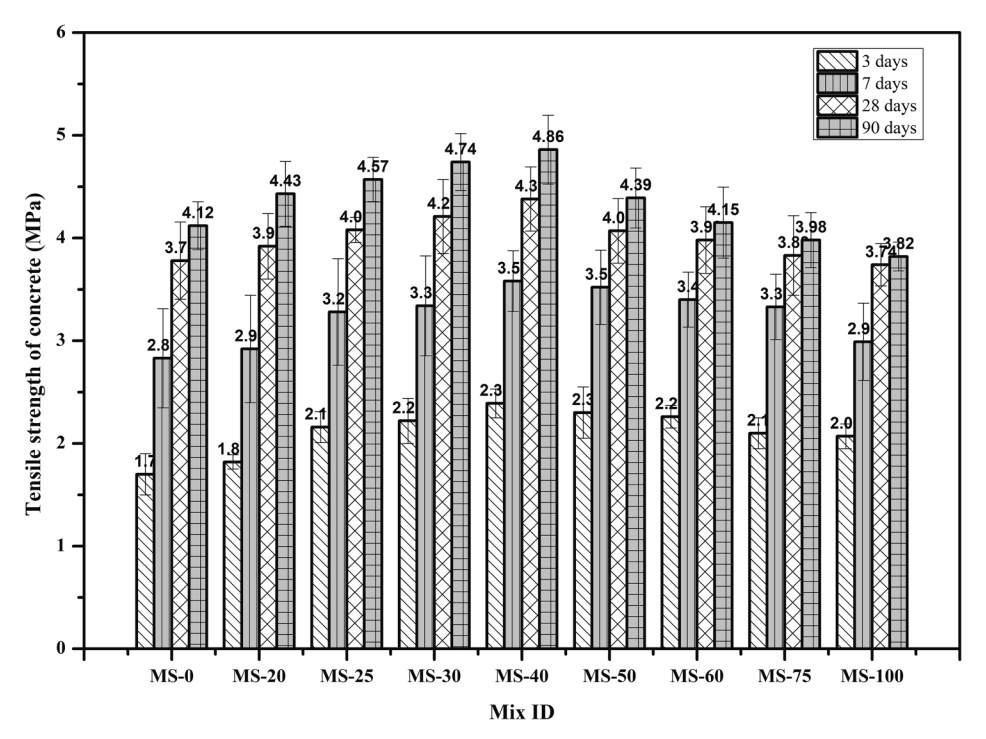


Fig. 10. Tensile strength of various mixes.

Ultrasonic pulse velocity

The UPV is typically used as a quality indicator for non-destructive testing of the specimen and can calculate the structural compactness based on the ultrasonic transit time. The variation of UPV with reference to curing ages is shown in Fig. 11. It is observed that with the increase in slag content, the UPV value decreases. This is because the sample expanded and developed pores because of the increased slag sand content, thus, lowering the UPV. However, the UPV values are observed to improve with increased curing ages for all mortar mixes. The slow chemical reaction during the early curing stages causes the UPV grows slowly. All the mixes exhibited the moderate range of UPV resulting in compact structure. The chemical reaction created by late-stage materials fills the test body's pores, improving the sample's compactness. Her-Yung Wang et al. (2022) also investigated that as specimen's pores increased, and the UPV decreased as the W/B ratio was raised. Therefore, the UPV and compressive strength exhibit the same pattern.

Correlation of various properties of slag sand induced concrete

The statistical correlation measure describes the magnitude and trend of a relationship between two or more variables, which is expressed as a number. Regression represents the relationship as an equation, whereas the relationship quantifies the strength of the linear correlation between two variables (Gokce et al., 2016; Ma et al., 2022). While nonlinear regression seeks to find a suitable nonlinear equation for this relationship, linear regression is a type of regression analysis in which a linear regression equation models the relationship between one or more independent and dependent variables. The nature and strength of the association between a dependent variable and several other independent variables are assessed using linear regression. It aids in the development of predictive models.

There needs to be more literature correlating various properties of slag sand-induced concrete. Hence in this study, regression analysis has been conducted using origin pro software (H.M. and Unnikrishnan,

2023) to find the correlation between various properties of concrete, such as workability, compressive strength (CS), split tensile strength (TS), and ultrasonic pulse velocity (UPV). F-statistic, mean square, p-value, and degree of freedom (DOF) are used in ANOVA to interpret the relationship between the variables (Venkatesan et al., 2019). Table 2 represents linear regression analysis of various properties of slag sand concrete.

Correlation between fresh and mechanical properties with the slag sand

This section describes the relationship between concrete properties and slag sand replacement. As discussed in the results & discussion section, workability, compressive strength, and split tensile strength increase up to 40 % replacement of slag sand and decrease gradually. This upward and downward trend is analyzed using linear regression separately, and the results are presented in Table 2 & 3. Figs. 12, 13, and 14 depicts the correlation between slag sand quantity with slump value, compressive strength, and tensile strength, respectively. The results indicated a decent correlation among the comparison made with R² values 0.76, 0.743, and 0.89 in the upward trend and 0.81, 0.656, and 0.78 in the downward trend, respectively. Our regression model fits the data more closely than the model with no independent variables because the F-statistic, also known as F-Value, is more significant in our analysis than the P-value for all correlations. The lower mean square suggests the closeness of the estimated values with actual values. DOF represents the number of observations or data used to fit the model as studied by Rashad et al. (n.d.), Mocharla et al. (2022), Wang et al. (2022).

Relationship of compressive strength versus split tensile strength

The proposed model for the relationship between split tensile strength (TS) and compressive strength (CS) of slag sand replaced concrete is represented in Fig. 15. The suggested model equations emerged for mean compressive strengths ranging from 45 MPa to 65 MPa are as follows.

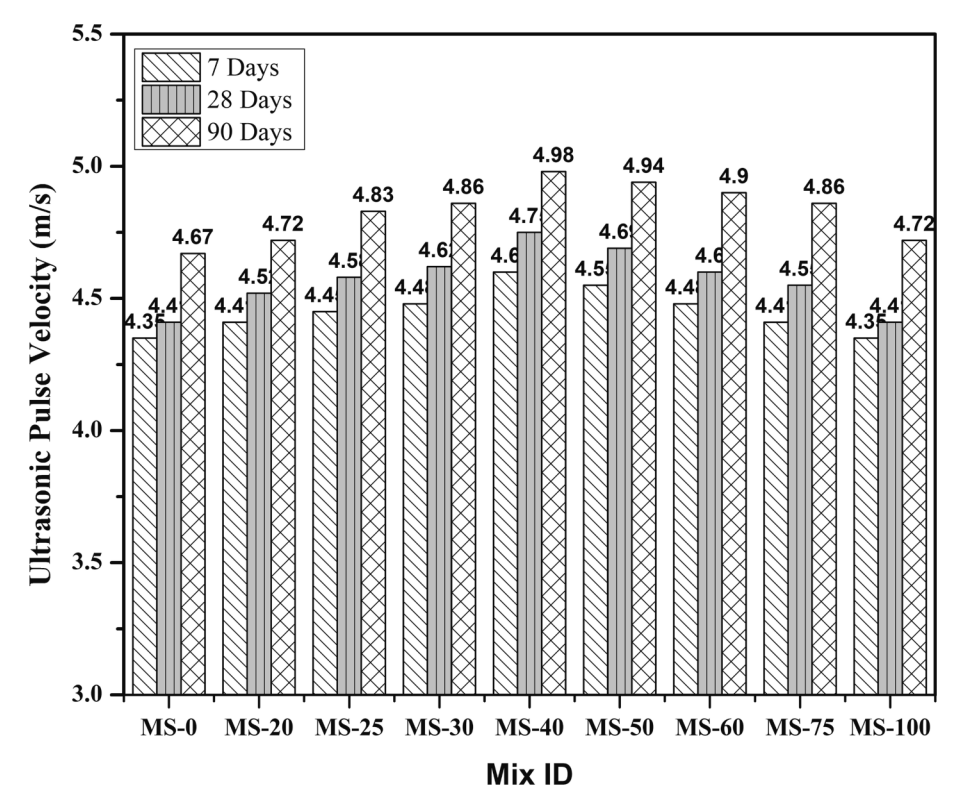


Fig. 11. UPV test results of various concrete.

Table 2Linear regression analysis of various properties of slag sand concrete.

Particular	Variation	Intercept	Slope	Statistics						_
		Value	Error	Value	Error	R^2	F- Value	Mean square	DOF	P-
Value										
CS v/s TS (Fig. 16)	Positive	2.18	0.16474	0.0348	0.00313	0.939	123.56	0.33264	7	0.0000
CS v/s UPV (Fig. 15)	Positive	3.54	0.05451	0.0205	0.00104	0.981	414.26	0.12937	7	0.0000
Slag Sand v/s CS (Fig. 14)	Positive	45.87	2.86854	0.3833	0.10804	0.743	12.59	129.29322	3	0.0382
	Negative	70.09	6.37672	-0.2740	0.09336	0.656	8.62	165.24941	3	0.0607
Slag Sand v/s TS (Fig. 13)	Positive	3.72	0.07044	0.0152	0.00265	0.889	32.9	0.20374	3	0.0105
	Negative	4.63	0.17012	-0.0097	0.00249	0.778	15.04	0.20526	3	0.0304
Slag Sand v/s Slump value (Fig. 12)	Positive	86.86	3.85453	0.5364	0.14517	0.76	13.65	253.16364	3	0.0344
	Negative	123.79	5.76971	-0.3568	0.08447	0.808	17.84	280.10227	3	0.0243

Table 3Correlation equations obtained after linear regression analysis.

Particular (X v/s Y)	Variation	Correlation Equation	R ²	Reference
CS v/s TS	Positive	$\begin{array}{l} Y = 2.177 + 0.034 \\ \times \ X \end{array}$	0.939	(Chithra et al., 2016)
CS v/s UPV	Positive	$Y = 3.4765 + 0.0217 \times X$	0.981	(Alakara et al., 2022)
Slag Sand v/s CS	Positive	$Y = 45.87 + 0.3833 \times X$	0.743	(Rashad, n.d.)
	Negative	$Y = 70.0884-0.2741 \times X$	0.656	
Slag Sand v/s TS	Positive	$Y = 3.724 + 0.0152 \times X$	0.889	(Chiew, 2019) (Rashad, n.d.)
	Negative	$ \begin{array}{l} Y = 4.628 0.0097 \\ \times \ X \end{array} $	0.778	
Slag Sand v/s Slump value	Positive	$Y = 86.864 + 0.5364 \times X$	0.76	(Rashad, n.d.)
	Negative	$\begin{array}{l} Y = 123.79 0.3568 \\ \times \ X \end{array}$	0.808	

$$TS = 2.177 + 0.034*CS$$

The proposed model's coefficient of determination (R²) demonstrated a 94 % fit to predict the relationship between CS and TS. Similar observations were made by using multiple linear regression analyses for various slag content and strengths prediction by Xue et al. (2022), Chithra et al. (2016), Dong et al. (2022).

Relationship of UPV versus compressive strength

The proposed model for the relationship between split tensile strength and compressive strength of slag sand replaced concrete is shown in Fig. 16. The suggested model equations, developed for mean

compressive strengths ranging from 45 MPa to 65 MPa, are as follows.

$$UPV = 3.4765 + 0.0217 \times CS$$

The proposed model's coefficient of determination (R^2) demonstrated a 98 % fit to predict the relationship between CS and UPV. Similar observations were made using multiple linear regression analyses for various slag content and strengths prediction by Chiew et al. (Chiew, 2019).

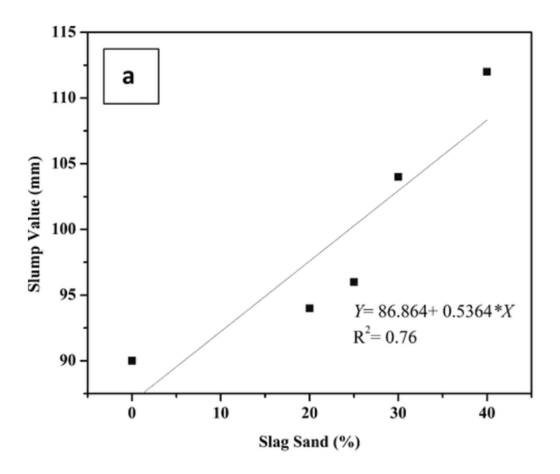
The following section describes the microstructural investigation results comprising SEM, EDS, and XRD and their interpretation concerning the mechanical properties test variation.

Microstructure properties of slag induced concrete

SEM and EDS

Scanning electron microscopy (SEM) and Energy dispersive analysis (EDS) is conducted using CARL ZEISS Sigma with Gemini Column having resolution of 1.5 nm and BRUKER Nano X-Flash Detector machine. The concrete specimens cured for 28 days are tested for strength and then the core sample size around 5 mm is chosen for SEM testing to rate the polymerization and structural elements in the matrix mix. Fig. 17 represents the SEM images and EDS of various concrete mix.

SEM clearly represents the presence of dense calcium silicate hydrate (CSH), needle shaped ettringite (CASH), cubical smooth structure of portlandite (CH) and enriched calcite formation in its internal structure that is mainly responsible for the strength attainment. Also, we can notice the presence of voids as black spots within the structure. The existence of CSH and CASH gel formation after hydration were also derived from EDS results. These gels responsible for the greater bonding and predominantly for the greater strength as evidenced by Zhang et al. (Zhang et al., 2021). The presence of Calcium, Silicon, Oxygen along with Aluminium helps in the complete hydration of the cement matrix as



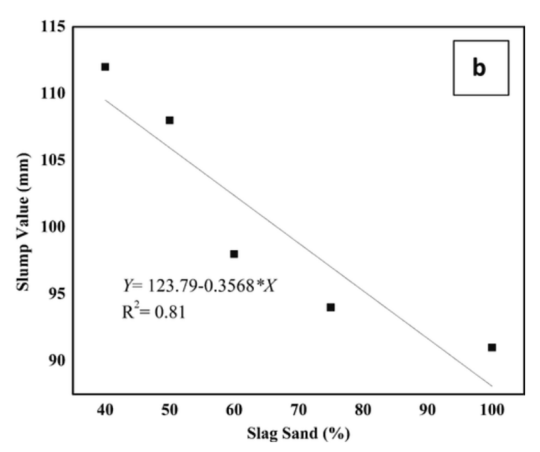


Fig. 12. Correlation between slump with slag sand content a) Positive variation b) Negative variation.

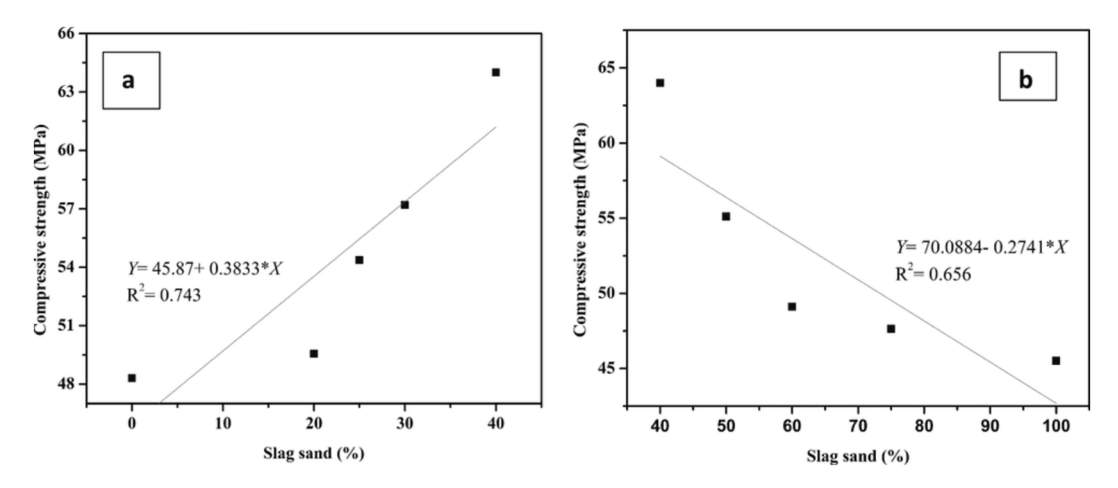


Fig. 13. Correlation between compressive strength with slag sand content a) Positive variation b) Negative variation.

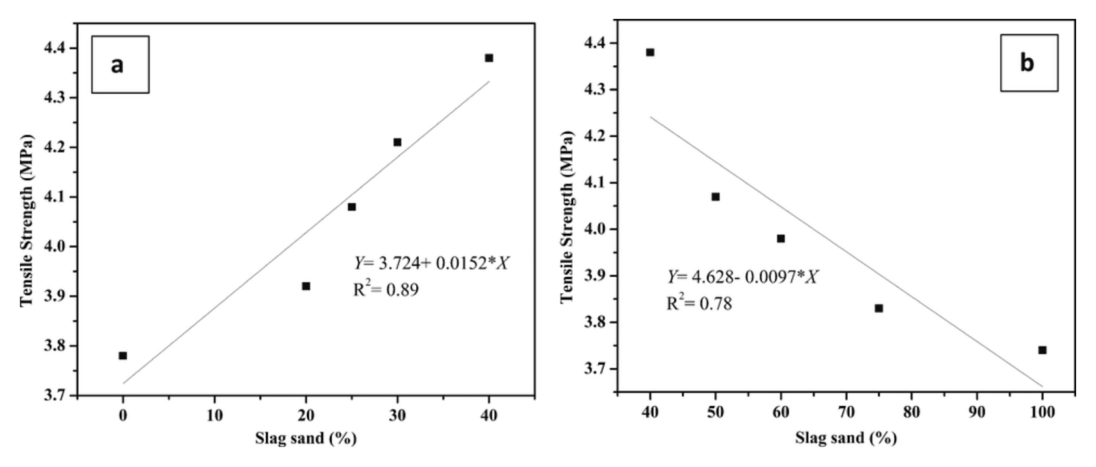


Fig. 14. Correlation between tensile strength with slag sand content a) Positive variation b) Negative variation.

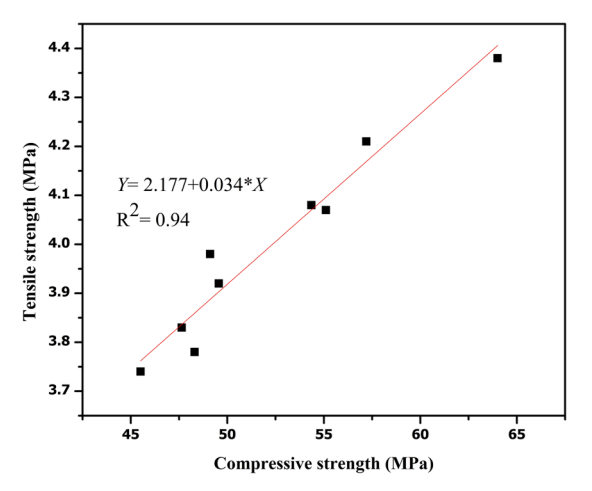


Fig. 15. Correlation between TS and CS.

evidenced in EDS test results of various concrete mixes. Also, we can notice the inter-facial transition zone (ITZ) between the binder materials with increased slag contents along with crack surfaces. The presence of sulfur, magnesium, un-hydrated aluminium results in the reduced strength and weaker matrix with increased pore structure as witnessed in Table 4.

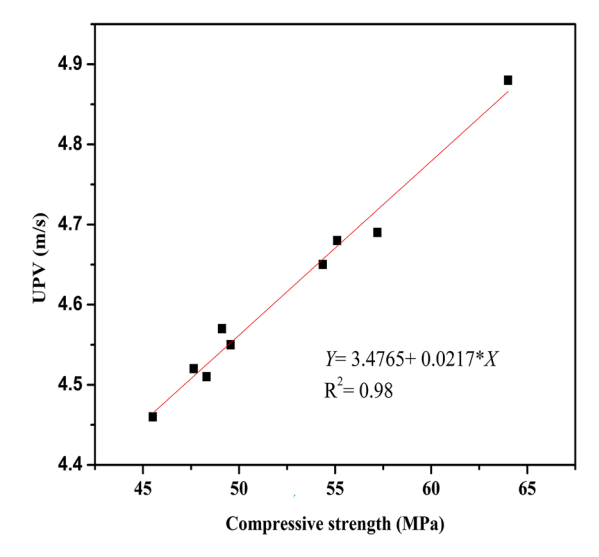


Fig. 16. Correlation between CS and UPV.

X-ray diffraction (XRD)

It is a vital method for the quantitative and qualitative analysis of samples of hydrated cement concrete. The XRD, based on Bragg's law was conducted on various concrete mix cured for 28 days. The broken specimen is crushed and sieved using 900 µm. Then this powder sample

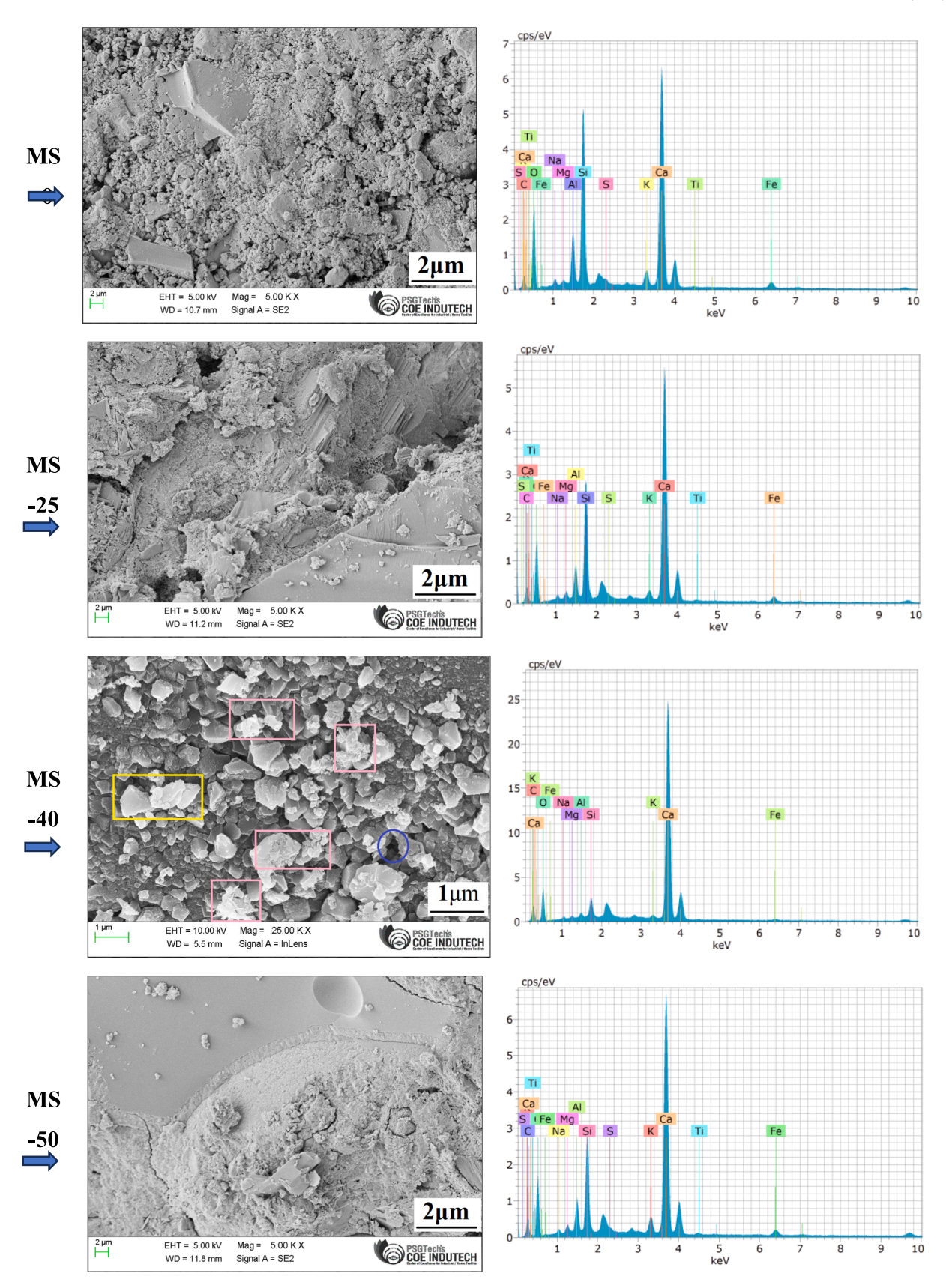


Fig. 17. SEM images & EDS of various concrete mixes.

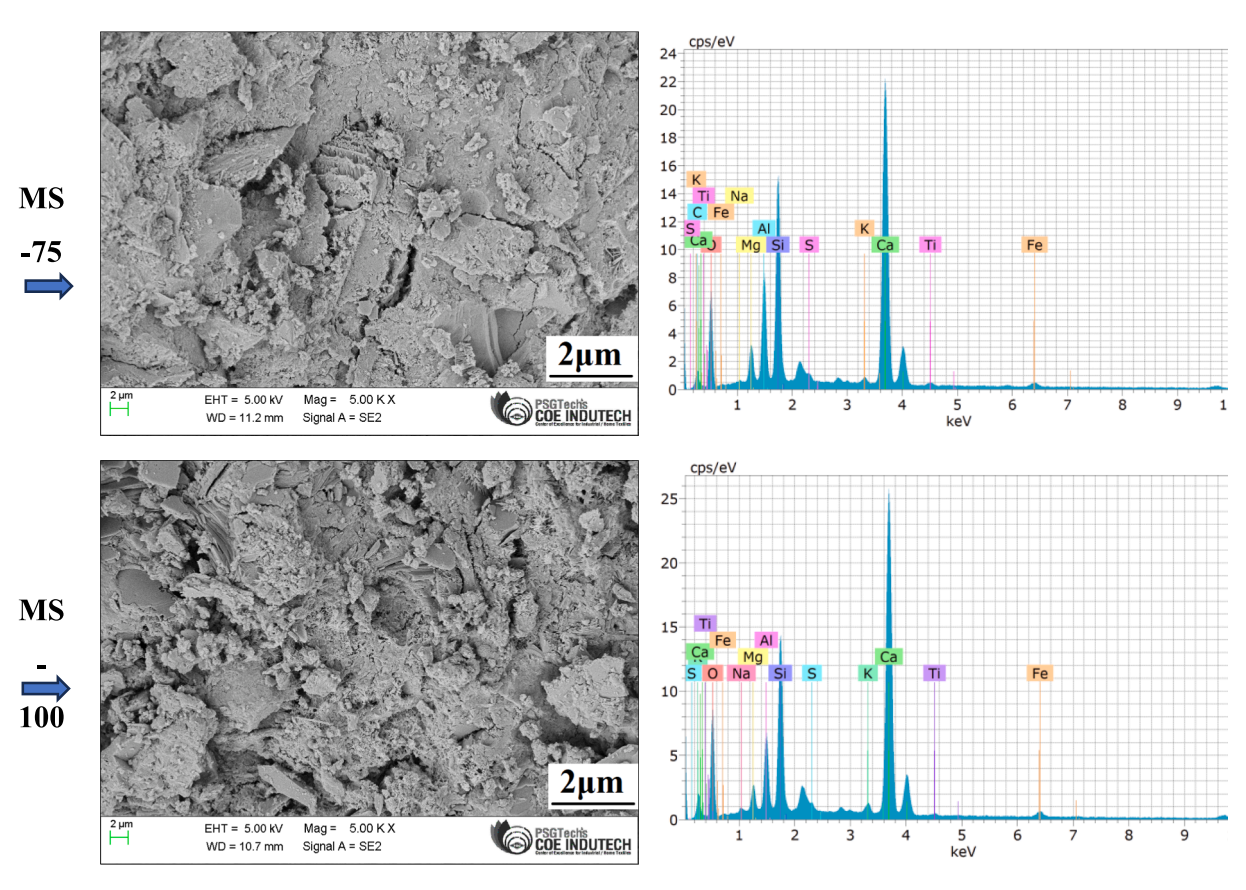


Fig. 17. (continued).

Table 4Atomic weights in percentage of the elements obtained in EDS test on various concrete mixes.

Elements	MS-0	MS-25	MS-40	MS-50	MS-75	MS-100
Calcium	16.64	20.09	45.31	20.71	18.10	20.86
Oxygen	57.04	56.15	51.09	55.76	53.66	65.03
Silicon	8.22	6.11	2.26	4.67	7.65	7.24
Iron	0.85	0.76	0.45	0.83	0.36	0.62
Aluminium	2.85	1.85	0.37	1.78	4.88	3.89
Magnesium	0.00	0.11	0.00	0.01	1.99	1.62
Sodium	0.46	0.13	0.31	0.00	0.15	0.25
Potassium	0.76	0.30	0.22	0.74	0.07	0.28
Carbon	13.00	14.41	0.00	15.36	12.93	0.00
Sulfur	0.11	0.00	0.00	0.00	0.16	0.22
Titanium	0.06	0.10	0.00	0.15	0.05	0.00

is tested. The test results of various slag induced concrete mixes are as shown in Fig. 18. All the concrete mixes have evidenced the presence of quartz, calcite, portlandite contributing strength to the concrete. From XRD of slag sand as shown in Fig. 4, we can notice the amorphous nature and crystalline nature for the artificial sand which results in dense matrix and increased strength with increased slag content. Also, industrial slag will be harder compared to artificial sand resulting in an enhanced strength. Quartz, basically silicon dioxide in the presence of calcium, oxygen, aluminium hydrated to form CSH and CASH gel and XRD peaks also evidenced the CSH (A), portlandite (B), calcite (C), quartz, and some portion of metal oxides composition present in the slag sand (Baalamurugan et al., 2021) in all the mixes of slag-induced concrete.

Subsequent section 9 and its subsections describe the durability test results and interpretation concerning microstructure and mechanical properties test results.

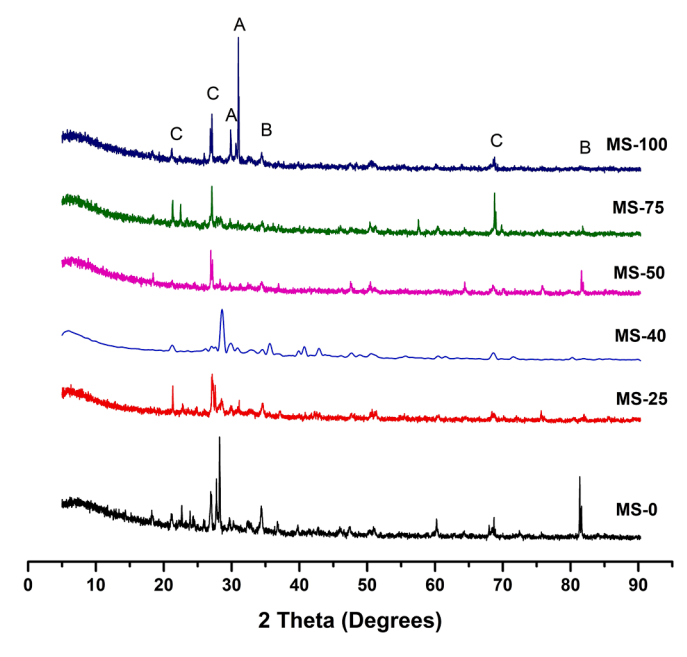


Fig. 18. XRD pattern of various concrete mix.

Durability of concrete

Rapid chloride penetration test (RCPT)

As per ASTM C 1202–2019, RCPT tests were performed on concrete specimens 100 mm in diameter and 50 mm thick. Table 5 displays the outcomes of RCPT tests conducted on various concrete mixtures. As per

Table 5RCPT test results of concrete specimens.

Mix ID	Total charge passed (Coulombs)	Chloride Ion Penetrability	Test method
MS-0	1314	Low	ASTM C
MS-20	1582	Low	1202-2019
MS-25	1788	Low	
MS-30	1804	Low	
MS-40	1836	Low	
MS-50	1862	Low	
MS-60	1876	Low	
MS-75	1894	Low	
MS-	1932	Low	
100			

the standards, the value ranges between 1000 and 2000, representing the low penetrability of chloride ions (Balasubramanian et al., 2021). The findings demonstrated that samples with higher slag sand contents are better resistant to salt ion penetration and facilitate salt ion resistance into the concrete surface, reducing corrosion. Slag sand's elements have little affinity for chloride ions, encouraging corrosion inhibition by reducing chloride ion penetration. From the microstructural test results, we can notice the strong matrix between the binders which enhances the durability of the concrete.

Carbonation depth

The carbonation depth is the average depth below the surface of the concrete at which carbon dioxide has reduced the alkalinity of the hydrated cement. The carbon penetration is tested after various curing times by misting the cured 70 mm cube specimens with 2 ml of 1 % phenolphthalein solution on the freshly broken surface (Santhosh et al., 2021)(Quedou et al., 2021). The average carbonation depth of different concrete mixtures at various curing times is shown in Fig. 19. According to the test investigation, there is a correlation between slag content and carbonation depth. As a result, increased slag content makes concrete surfaces less durable by encouraging corrosion on exposed surfaces.

Water absorption and sorptivity

The water absorption test is crucial for determining how durable and water-resistant the concrete is. It aids in ensuring that the concrete or mortar will function as expected in its intended setting. After 28 days of curing, specimens with 100 mm in diameter and 50 mm 5 mm in height

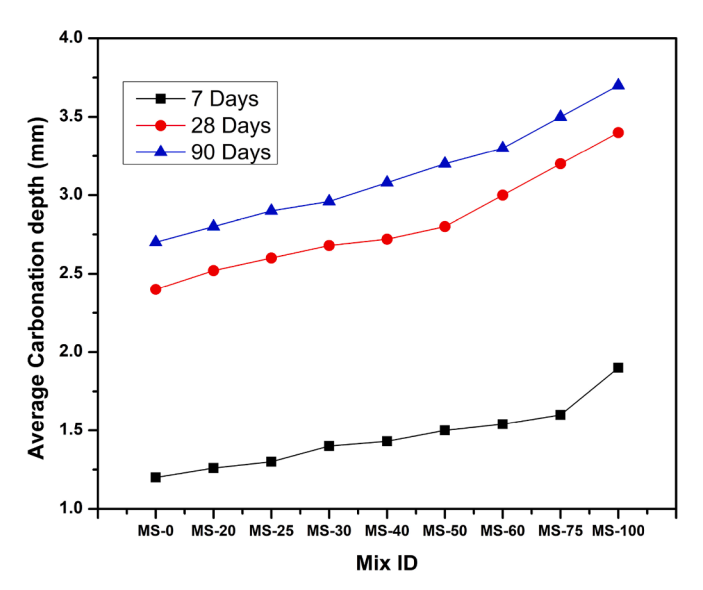


Fig. 19. Average carbonation depth of various concrete mixes.

were cast to undergo a water absorption test. Primary water absorption is noted, with the initial absorption lasting approximately 5 h. The absorption variation of different concrete mixes is shown in Fig. 20 (a). The absorption test results show that more slag increases water absorption and that slag sand replacement levels of 75 and 100 % produce the highest absorption levels compared to other mixtures.

According to ASTM C 3585 standards, the sorptivity test can measure how quickly a specimen is absorbed by capillary action and thus determine how well the structure is performing. After curing for 28 days, cylindrical samples measuring 100 mm in diameter and 60 mm in thickness were used for the sorptivity test. After five hours of exposure, the saturated calcium hydroxide solution's high initial absorption levels stabilize. As shown in Fig. 20 (b), the trend follows that of water absorption tests, rising with higher slag sand content. Maximum absorption is observed when slag sand is replaced by 100 %.

The sorptivity v/s percentage water absorption of different concrete mixes is shown in Fig. 20(c). Sorptivity rises as slag sand content increases, and this can be seen in the sorptivity range of 0.17 to 0.24 kg/ $m^2h^{0.5}$.

Impact resistance

After 28 days of curing, an impact resistance test was conducted on specimens measuring 100 mm in diameter and 60 mm in height to determine the durability and compactness of the concrete. The impact resistance is calculated using the number of blows needed to break the specimens (Suganya et al., 2018). Fig. 21 shows the impact resistance variation for various slag sand mixes. Increased impact resistance is the result of dense matrix between the concrete ingredients. Microstructure test results, compressive strength and UPV tests resulted in strong matrix and better load resisting capacity. Industry by-product slag sand found be harder than artificial sand, results in an increased resistance to sudden loads. The test results demonstrate that slag sand-mixed concrete is more impact-resistant than conventional concrete (Carvalho Eugênio et al., 2021). The slag sand helps absorb the impact energy due to better bond formation and hydration with cement and coarse aggregates (Al-Hadithi et al., 2019; Gupta et al., 2019).

Chemical salts exposure

A durability test of chemical salt exposure is performed on concrete mixes by immersing them in 1 N NaCl, Na₂SO₄, and MgSO₄ salts for 28 days. Then these specimens were dried and tested for compressive strength using CTM. The results indicated a marginal reduction in compressive strength in all the mixes around 3 MPa to 15 MPa compared to water curing. Fig. 22 represents the effect of chemical salts on the strength of various concrete mixes. Sulfate salts exposed specimens resulted in a higher reduction in compressive strength than chloride salt exposure. This effect of sulfate is due to the disintegration, expansion, and crack formation on the surface of the concrete. Also, the authors noticed less difference in strength reduction with varied percentages of slag sand due to salts exposure than conventional mix.

Section 10 expresses the cost analysis incurred in concrete preparation per m^3 quantity of concrete, referring to its comparison with M-sand and Slag sand.

Cost analysis of slag induced concrete (Kg/m³)

Table 6 represents slag/ M—sand induced concrete cost analysis in kg/m^3 . The calculations show that adding slag sand can be better than M—sand in concrete. Meanwhile, slag sand can reduce the disposal challenge and the burden on the environment, providing better utilization of industrial effluent. Construction location plays a significant role in reducing the cost of concrete production. This analysis considers the material cost encountered in our laboratory's experimental investigation, including transportation expenses. Hence, slag sand is found to

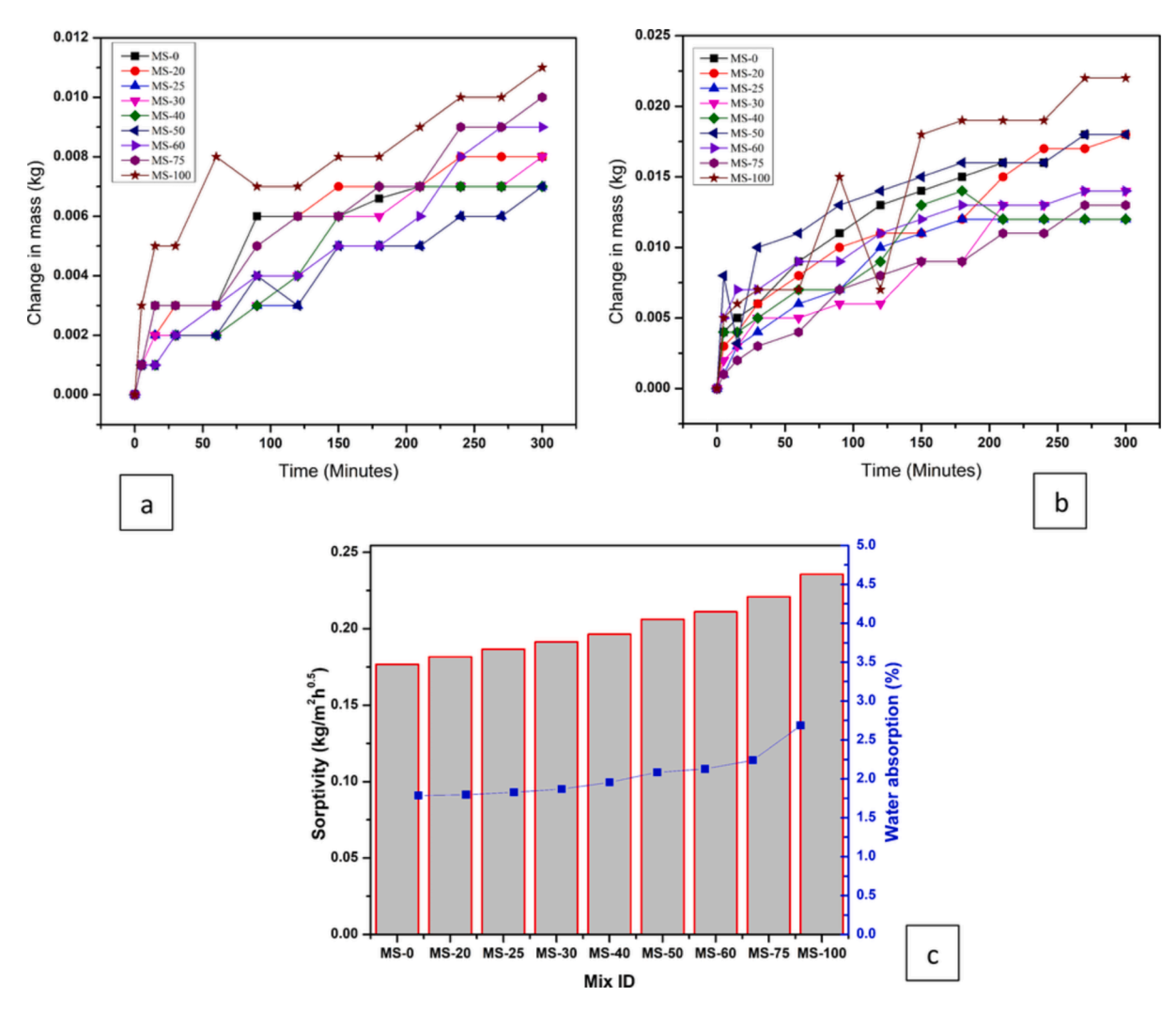


Fig. 20. Test results of a) Water absorption b) Sorptivity c) Sorptivity v/s water absorption of various mixes.

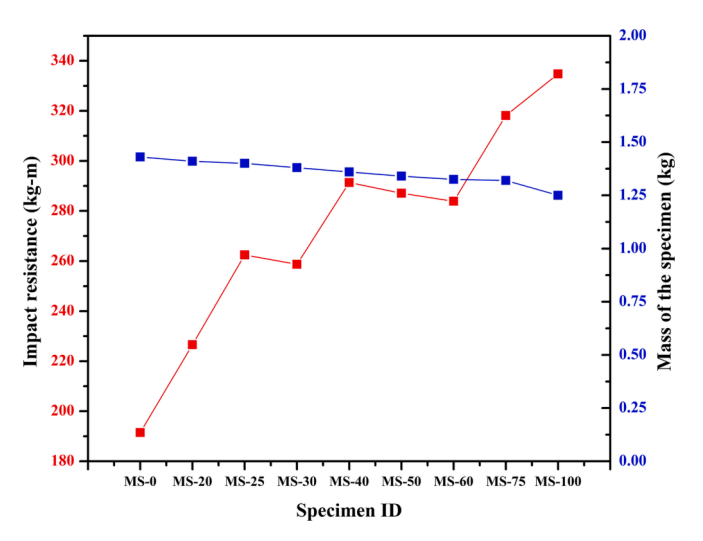


Fig. 21. Impact resistance variation of concrete specimens.

be beneficial in utilizing it for construction activities.

Conclusion

Slag sand, a steel industry by-product produced by JSW steel plant

Ballari, is investigated by replacing fine aggregate with slag sand. Microstructure, fresh, mechanical and durability properties are investigated & studied to determine their optimum replacement level to minimize the disposal challenge and environmental pollution. After the successful experimental investigation on slag sand-induced concrete, the following conclusions were made based on the empirical study.

- Workability improves with increasing slag sand up to an optimal level, beyond which workability decreases due to higher water absorption of slag sand. Medium to high workability is observed in slag sand-incorporated concrete with a true and shear slump.
- Compressive and tensile strength increase with increased slag sand replacement due to the dense formation of CSH, CASH, and CH with reduced pores, as evidenced in microstructural test results. Beyond 40 % of slag sand replacement, strength starts declining due to increased water absorption of slag sand at the early ages, which later turns to void formations.
- Microstructure and Non-destructive testing of UPV test results indicate the dense structure and strong matrix between concrete ingredients, resulting in significant improvement at 40 % replacement of slag sand. Thereafter, we noticed an increased water absorption as revealed from the water absorption test, resulting in improved porous structure and incomplete hydration of cementitious material, which decreased mechanical properties.



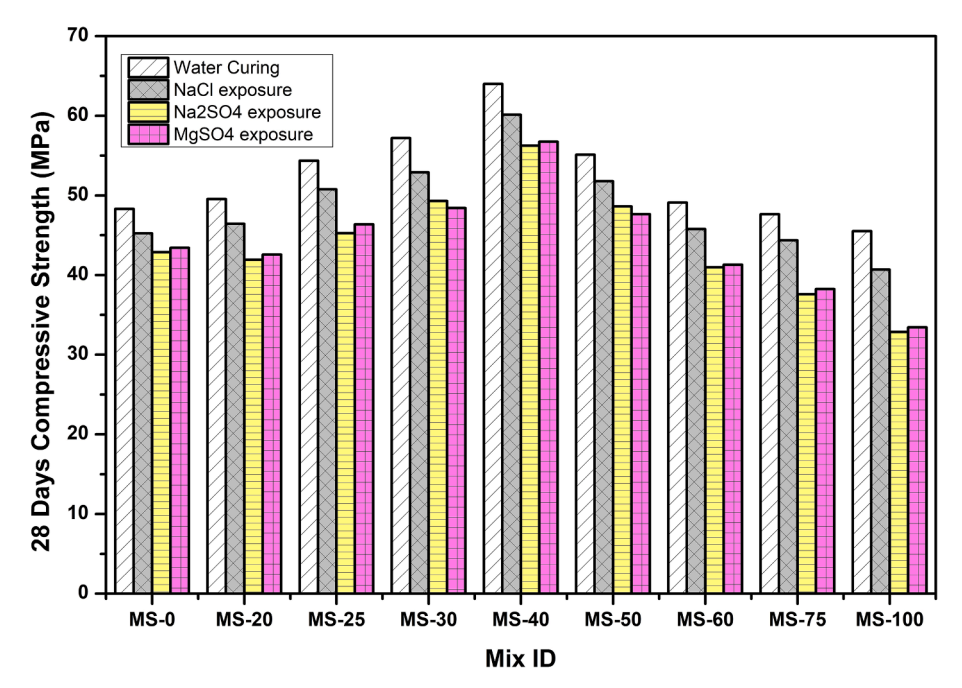


Fig. 22. Effect of chemical salts exposure on the compressive strength of concrete mixes.

Table 6Cost analysis of Slag/ M-sand induced concrete (kg/m³).

Sl. No.	Material	Per unit cost (Rs/kg)	Qty (per m ³)	Cost (Rs) with M-sand	Cost (Rs) with Slag- sand
1	Cement	16	388	6208	6208
2	Slag Sand	2.5	489	0	1222
3	M-Sand	3	489	1467	0
4	Coarse aggregate	3	1173	3519	3519
5	Superplasticizer	200	2.328	465	465
Total	Rate/Qty (per m ³)	224.5	2541.328	11,659	11,414

- Regression analysis revealed a strong correlation between various properties of concrete with the replacement of slag sand, and the proposed model equations align with the experimental data.
- Durability tests on concrete showed increased absorption, penetration of chloride ions, and carbonation depth, resulting in reduced strength and expanded pores in the structure. However, increased slag sand content in the concrete improved the shock absorption and showed higher resistance to crack formation. Chemical salt exposure showed similar performance in all mixes with a marginal decline in strength. Notably, sulfate salts exposed specimens have evidenced a significant reduction in strength compared to chloride salt exposure.
- The cost analysis indicates slag sand-induced concrete is economically better than artificial sand mixed concrete, contributing to cost reduction by recycling industrial effluent in concrete production. Thus, replacing slag sand as a fine aggregate in concrete is beneficial for strength gain. Using waste industrial by-products like slag sand in concrete reduces the disposal challenges and cost of concrete and manages the waste effectively by producing sustainable and ecofriendly concrete.

Declaration of competing interest

The authors declare that they have no known competing financial interests or personal relationships that could have appeared to influence the work reported in this paper.

Data availability

No data was used for the research described in the article.

Acknowledgement

Authors Would like to thank GITAM University, Bengaluru for their constant support and encouragement for carrying out research work.

Funding

The authors declare that no funds, grants, or other support were received during the preparation of this research work.

It will be available based on reasonable request to the corresponding author.

REFERENCES

Alakara, E.H., Nacar, S., Sevim, O., Korkmaz, S., Demir, I., 2022. Determination of compressive strength of perlite-containing slag-based geopolymers and its prediction using artificial neural network and regression-based methods. Constr. Build. Mater. 359, 129518 https://doi.org/10.1016/j.conbuildmat.2022.129518.

Al-Hadithi, A.I., Noaman, A.T., Mosleh, W.K., 2019. Mechanical properties and impact behavior of PET fiber reinforced self-compacting concrete (SCC). Compos. Struct. 224, 111021 https://doi.org/10.1016/j.compstruct.2019.111021.

Arribas, I., Santamaría, A., Ruiz, E., Ortega-López, V., Manso, J.M., 2015. Electric arc furnace slag and its use in hydraulic concrete. Constr. Build. Mater. 90, 68–79. https://doi.org/10.1016/j.conbuildmat.2015.05.003.

Baalamurugan, J., Kumar, V.G., Chandrasekaran, S., Balasundar, S., Venkatraman, B., Padmapriya, R., Raja, V.K.B., 2021. Recycling of steel slag aggregates for the development of high density concrete: Alternative & environment-friendly radiation shielding composite. Compos. Part B Eng. 216, 108885 https://doi.org/10.1016/j. compositesb.2021.108885.

Balasubramanian, B., Gopala Krishna, G.V.T., Saraswathy, V., Srinivasan, K., 2021. Experimental investigation on concrete partially replaced with waste glass powder and waste E-plastic. Constr. Build. Mater. 278, 122400 https://doi.org/10.1016/j. conbuildmat.2021.122400.

Carvalho Eugênio, T.M., Francisco Fagundes, J., Santos Viana, Q., Pereira Vilela, A., Farinassi Mendes, R., 2021. Study on the feasibility of using iron ore tailing (iot) on technological properties of concrete roof tiles. Constr. Build. Mater. 279 https://doi.org/10.1016/j.copbuildmat.2021.122484.

Chiew, F.H., 2019. Prediction of blast furnace slag concrete compressive strength using artificial neural networks and multiple regression analysis. Proc. - 2019 Int. Conf. Comput. Drone Appl. Iconda 2019, 54–58. https://doi.org/10.1109/ IConDA47345.2019.9034920.

- Chithra, S., Kumar, S.R.R.S., Chinnaraju, K., Alfin Ashmita, F., 2016. A comparative study on the compressive strength prediction models for High Performance Concrete containing nano silica and copper slag using regression analysis and Artificial Neural Networks. Constr. Build. Mater. 114, 528–535. https://doi.org/10.1016/j. conbuildmat.2016.03.214.
- Dong, J., Xie, H., Dai, Y., Deng, Y., 2022. Prediction Model of Compressive Strength of Fly Ash-Slag Concrete Based on Multiple Adaptive Regression Splines. Open J. Appl. Sci. 12, 284–300. https://doi.org/10.4236/ojapps.2022.123021.
- Gencel, O., Karadag, O., Oren, O.H., Bilir, T., 2021. Steel slag and its applications in cement and concrete technology: A review. Constr. Build. Mater. 283, 122783 https://doi.org/10.1016/j.conbuildmat.2021.122783.
- Gokce, A., Beyaz, C., Ozkan, H., 2016. Influence of fines content on durability of slag cement concrete produced with limestone sand. Constr. Build. Mater. 111, 419–428. https://doi.org/10.1016/j.conbuildmat.2016.02.139.
- Gupta, T., Kothari, S., Siddique, S., Sharma, R.K., Chaudhary, S., 2019. Influence of stone processing dust on mechanical, durability and sustainability of concrete. Constr. Build. Mater. 223, 918–927. https://doi.org/10.1016/j.conbuildmat.2019.07.188.
- H.M., T., Unnikrishnan, S.,, 2022. Utilization of industrial and agricultural waste materials for the development of geopolymer concrete- A review. Mater. Today Proc. 65, 1290–1297. https://doi.org/10.1016/j.matpr.2022.04.192.
- H.M., T., Unnikrishnan, S.,, 2023. Mechanical Strength and Microstructure of GGBS-SCBA based Geopolymer Concrete. J. Mater. Res. Technol. 24, 7816–7831. https:// doi.org/10.1016/j.jmrt.2023.05.051.
- IS 516, 1959. Method of Tests for Strength of Concrete. Bur. Indian Stand. 1-30.
- Jiang, Y., Ling, T.-C., Shi, C., Pan, S.-Y., 2018. Characteristics of steel slags and their use in cement and concrete—A review. Resour. Conserv. Recycl. 136, 187–197. https://doi.org/10.1016/j.resconrec.2018.04.023.
- Jiang, X., Xiao, R., Bai, Y., Huang, B., Ma, Y., 2022. Influence of waste glass powder as a supplementary cementitious material (SCM) on physical and mechanical properties of cement paste under high temperatures. J. Clean. Prod. 340, 130778 https://doi. org/10.1016/j.jclepro.2022.130778.
- Jiang, X., Zhang, Y., Zhang, Y., Ma, J., Xiao, R., Guo, F., Bai, Y., Huang, B., 2023. Influence of size effect on the properties of slag and waste glass-based geopolymer paste. J. Clean. Prod. 383, 135428 https://doi.org/10.1016/j.jclepro.2022.135428.
- Kourounis, S., Tsivilis, S., Tsakiridis, P.E., Papadimitriou, G.D., Tsibouki, Z., 2007. Properties and hydration of blended cements with steelmaking slag. Cem. Concr. Res. 37, 815–822. https://doi.org/10.1016/j.cemconres.2007.03.008.
- Lai, M.H., Zou, J., Yao, B., Ho, J.C.M., Zhuang, X., Wang, Q., 2021. Improving mechanical behavior and microstructure of concrete by using BOF steel slag aggregate. Constr. Build. Mater. 277, 122269 https://doi.org/10.1016/j. conbuildmat.2021.122269.
- Lai, M.H., Chen, Z.H., Wang, Y.H., Ho, J.C.M., 2022. Effect of fillers on the mechanical properties and durability of steel slag concrete. Constr. Build. Mater. 335 https://doi. org/10.1016/j.conbuildmat.2022.127495.
- Li, H., Schamel, E., Liebscher, M., Zhang, Y., Fan, Q., Schlachter, H., Köberle, T., Mechtcherine, V., Wehnert, G., Söthje, D., 2023. Recycled carbon fibers in cement-based composites: Influence of epoxide matrix depolymerization degree on interfacial interactions. J. Clean. Prod. 411, 137235 https://doi.org/10.1016/j.jclepro.2023.137235.
- Lu, D., Huo, Y., Jiang, Z., Zhong, J., 2023a. Carbon nanotube polymer nanocomposites coated aggregate enabled highly conductive concrete for structural health monitoring. Carbon n. y. 206, 340–350. https://doi.org/10.1016/j. carbon 2023 02 043
- Lu, D., Jiang, X., Leng, Z., Zhang, S., Wang, D., Zhong, J., 2023b. Dual responsive microwave heating-healing system in asphalt concrete incorporating coal gangue and functional aggregate. J. Clean. Prod. 422, 138648 https://doi.org/10.1016/j. jclepro.2023.138648.
- Lu, D., Jiang, X., Tan, Z., Yin, B., Leng, Z., Zhong, J., 2023c. Enhancing sustainability in pavement Engineering: A-state-of-the-art review of cement asphalt emulsion mixtures. Clean. Mater. 9, 100204 https://doi.org/10.1016/j.clema.2023.100204.
- Lu, D., Wang, D., Wang, Y., Zhong, J., 2023d. Nano-engineering the interfacial transition zone between recycled concrete aggregates and fresh paste with graphene oxide. Constr. Build. Mater. 384, 131244 https://doi.org/10.1016/j. conbuildmat.2023.131244.
- Ma, Q., Shi, Y., Xu, Z., Ma, D., Huang, K., 2022. Research on a multivariate non-linear regression model of dynamic mechanical properties for the alkali-activated slag mortar with rubber tire crumb. Case Stud. Constr. Mater. 17, e01371.

- Mo, K.H., Thomas, B.S., Yap, S.P., Abutaha, F., Tan, C.G., 2020a. Viability of agricultural wastes as substitute of natural aggregate in concrete: A review on the durability-related properties. J. Clean. Prod. 275, 123062 https://doi.org/10.1016/J. JCLEPRO 2020 123062
- Mo, L., Yang, S., Huang, B., Xu, L., Feng, S., Deng, M., 2020b. Preparation, microstructure and property of carbonated artificial steel slag aggregate used in concrete. Cem. Concr. Compos. 113, 103715 https://doi.org/10.1016/j. cemconcomp.2020.103715.
- Mocharla, I.R., Selvam, R., Govindaraj, V., Muthu, M., 2022. Performance and life-cycle assessment of high-volume fly ash concrete mixes containing steel slag sand. Constr. Build. Mater. 341, 127814 https://doi.org/10.1016/j.conbuildmat.2022.127814.
- Nalon, G.H., Santos, R.F., de Lima, G.E.S., Andrade, I.K.R., Pedroti, L.G., Ribeiro, J.C.L., Franco de Carvalho, J.M., 2022. Recycling waste materials to produce self-sensing concretes for smart and sustainable structures: A review. Constr. Build. Mater. 325, 126658 https://doi.org/10.1016/J.CONBUILDMAT.2022.126658.
- Quedou, P.G., Wirquin, E., Bokhoree, C., 2021. Sustainable concrete: Potency of sugarcane bagasse ash as a cementitious material in the construction industry. Case Stud. Constr. Mater. 14, e00545.
- Reshma, T.V., Manjunatha, M., Sankalpasri, S., Tanu, H.M., 2021. Effect of waste foundry sand and fly ash on mechanical and fresh properties of concrete. Mater. Today Proc. 10.1016/j.matpr.2020.12.821.
- Santhosh, K.G., Subhani, S.M., Bahurudeen, A., 2021. Cleaner production of concrete by using industrial by-products as fine aggregate: A sustainable solution to excessive river sand mining. J. Build. Eng. 42, 102415 https://doi.org/10.1016/j. iphs.2021.102415
- Sithole, N.T., Tsotetsi, N.T., Mashifana, T., Sillanpää, M., 2022. Alternative cleaner production of sustainable concrete from waste foundry sand and slag. J. Clean. Prod. 336 https://doi.org/10.1016/j.jclepro.2022.130399.
- Suganya, M., Sathyan, D., Mini, K.M., 2018. Performance of Concrete Using Waste Fiber Reinforced Polymer Powder as a Partial Replacement for Fine Aggregate. Mater. Today Proc. 5, 24114–24123. https://doi.org/10.1016/j.matpr.2018.10.205.
- T.V., R., Chandan Kumar, P., 2023. Effect of slag sand as river sand and its influence on compressive strength of the cement mortar. Mater. Today Proc. 10.1016/j. matpr.2023.03.136.
- Teja, C., Naidu, D.A., Venkateswarlu, D., 2020. Performance of copper slag as replacement of fine aggregate with different grades. J Crit. Rev. 7, 731–735. https://doi.org/10.31838/jcr.07.09.141.
- Teng, S., Lim, T.Y.D., Sabet Divsholi, B., 2013. Durability and mechanical properties of high strength concrete incorporating ultra fine Ground Granulated Blast-furnace Slag. Constr. Build. Mater. 40, 875–881. https://doi.org/10.1016/j. conbuildmat.2012.11.052.
- Venkatesan, M., Zaib, Q., Shah, I.H., Park, H.S., 2019. Optimum utilization of waste foundry sand and fly ash for geopolymer concrete synthesis using D-optimal mixture design of experiments. Resour. Conserv. Recycl. 148, 114–123. https://doi.org/ 10.1016/j.resconrec.2019.05.008.
- Wang, X., Lu, X., Turvey, C.C., Dipple, G.M., Ni, W., 2022b. Evaluation of the carbon sequestration potential of steel slag in China based on theoretical and experimental labile Ca. Resour. Conserv. Recycl. 186, 106590 https://doi.org/10.1016/j. resconrec.2022.106590.
- Wang, H.Y., Tsai, S.L., Hung, C.C., Jian, T.Y., 2022a. Research on engineering properties of cement mortar adding stainless steel reduction slag and pozzolanic materials. Case Stud. Constr. Mater. 16, e01144.
- Xue, G., Fu, Q., Xu, S., Li, J., 2022. Macroscopic mechanical properties and microstructure characteristics of steel slag fine aggregate concrete. J. Build. Eng. 56, 104742 https://doi.org/10.1016/j.jobe.2022.104742.
- Rashad, A.M., n.d. Behavior of steel slag aggregate in mortar and concrete A comprehensive overview. J. Build. Eng. 53, 104536. 10.1016/j.jobe.2022.104536.
- Yu, Q., Zhu, B., Li, X., Meng, L., Cai, J., Zhang, Y., Pan, J., 2023. Investigation of the rheological and mechanical properties of 3D printed eco-friendly concrete with steel slag. J. Build. Eng. 72, 106621 https://doi.org/10.1016/j.jobe.2023.106621.
- Zhang, X., Zhao, S., Liu, Z., Wang, F., 2019. Utilization of steel slag in ultra-high performance concrete with enhanced eco-friendliness. Constr. Build. Mater. 214, 28–36. https://doi.org/10.1016/j.conbuildmat.2019.04.106.
- Zhang, X., Fang, H., Du, M., Shi, M., Zhang, C., 2021. Experimental Study on the Mechanical Properties of the Fiber Cement Mortar Containing Polyurethane. Adv. Mater. Sci. Eng. 2021, 1–18. https://doi.org/10.1155/2021/9956897.